



King Saud University
Journal of Saudi Chemical Society

www.ksu.edu.sa
www.sciencedirect.com



ORIGINAL ARTICLE

Synthesis, crystal structure and applications of palladium thiosalicylate complexes

S.B. Moosun^a, L.H. Blair^b, S.J. Coles^c, M.G. Bhowon^a, S. Jhaumeer-Laulloo^{a,*}

^a Department of Chemistry, Faculty of Science, University of Mauritius, Mauritius

^b Centre for Defence Chemistry, Cranfield University, Defence Academy of the United Kingdom, Shrivenham SN6 8LA, UK

^c Chemistry, Faculty of Natural & Environmental Sciences, University of Southampton, UK

Received 22 July 2015; revised 12 October 2015; accepted 14 October 2015

KEYWORDS

Thiobenzoate;
Palladium;
Heck;
Bacteria;
Radicals

Abstract Three palladium thiosalicylate complexes $[\text{Pd}(\text{tb})(\text{bipy})]\cdot 3\text{H}_2\text{O}$ (**1**), $[\text{Pd}_2(\text{tb})_2(\text{bipy})_2](\text{dtdb})_2$ (**2**) and $[\text{Pd}_2(\text{tb})_2(\text{phen})_2]\text{dtdb}\cdot\text{H}_2\text{O}$ (**3**) (bipy = bipyridine; phen = phenanthroline) were prepared from the reaction of $\text{PdCl}_2(\text{CH}_3\text{CN})_2$ with dithiosalicylic acid (dtdb) which underwent cleavage to form thiobenzoate anion (tb) in DMF/MeOH. Square planar geometries of the complexes with a N_2SO coordination type were proposed on the basis of single crystal X-ray structural study. The presence of trapped and uncoordinated dtdb was observed in complexes **2** and **3**. Complexes **1–3** were evaluated as catalysts for Heck coupling reactions of methyl acrylate with iodobenzene, and showed moderate activities at a very low catalyst loading. Complex **1** was found to inhibit the growth of bacteria and scavenge free radicals efficiently.

© 2015 King Saud University. Production and hosting by Elsevier B.V. This is an open access article under the CC BY-NC-ND license (<http://creativecommons.org/licenses/by-nc-nd/4.0/>).

1. Introduction

Heck reactions are known to play significant roles in modern synthetic chemistry for C–C bond formation and involve the coupling of an aryl, vinyl halide or sulfonate with an alkene and are found to be versatile and applicable to a wide range of species [1,11,14]. Traditionally, Heck coupling reactions have been catalyzed by less stable and air sensitive phosphine based palladium complexes [8]. Hence, the study of more

stable and cheaper catalysts was of due importance. Mononuclear palladium complexes of carbenes [12], benzoxazoles [5], thiosemicarbazones [7] and pyridylimines [20] have been used as catalysts in Heck coupling reactions. Palladium-based carboxylate complexes have been reported to catalyze the oxidation of glucose to gluconic acid [13] or methoxycarbonylation of iodobenzene [27], but none of them have been used in Heck reactions. Moreover, palladium carboxylate complexes are known to possess interesting biological properties [3,16]. Gao et al. [9] reported the formation of $[\text{Pd}(\text{tb})\text{L}]\cdot m\text{H}_2\text{O}$ (**1**) (L = bipy, phen, $m = 1$ or 2) using a different reaction strategy and reactant which consists of stirring the coligands with thiosalicylic acid in the presence of $\text{K}_2[\text{PdCl}_4]$ at room temperature. In this regard, we have synthesized palladium complexes (**1–3**) derived from dithiosalicylic acid in the presence of bipyridine and phenanthroline that can lead to an efficient homogeneous catalyst in the conversion of aryl

* Corresponding author.

E-mail address: sabina@uom.ac.mu (S. Jhaumeer-Laulloo).

Peer review under responsibility of King Saud University.



Production and hosting by Elsevier

<http://dx.doi.org/10.1016/j.jscs.2015.10.003>

1319-6103 © 2015 King Saud University. Production and hosting by Elsevier B.V.

This is an open access article under the CC BY-NC-ND license (<http://creativecommons.org/licenses/by-nc-nd/4.0/>).

Please cite this article in press as: S.B. Moosun et al., Synthesis, crystal structure and applications of palladium thiosalicylate complexes, Journal of Saudi Chemical Society (2015), <http://dx.doi.org/10.1016/j.jscs.2015.10.003>

halides into Heck products at very low amounts of catalyst loading.

2. Results and discussions

2.1. Synthesis and characterization of the complexes

The palladium complexes **1** and **2** were synthesized by the slow diffusion of $\text{PdCl}_2(\text{CH}_3\text{CN})_2$ over dtdb in DMF/MeOH in the presence of bipy (Fig. 1). Complex **2** was obtained as a residue while crystals of **1** were isolated from the filtrate after a few weeks. When phen was used as co-ligand, orange crystals of **3** were formed but no product was obtained from its filtrate even after several months. The structures of the complexes were characterized by spectral (IR, NMR) and elemental analyses data and were further confirmed by X-ray data (Table 1). The spectral and physical data of complex **1** corroborated with previous reports [9]. The carboxylate asymmetric stretching bands in complexes **2** and **3** were found to be at 1619 and 1601 cm^{-1} , confirming the deprotonation and coordination of carboxylate oxygens in these to Pd complexes [18]. Additional carboxylate stretching was observed at 1667 and 1665 cm^{-1} in IR spectra of **2** and **3**, supporting the presence of uncoordinated trapped dtdb.

The S—S bonds in complexes **2** and **3** were shifted slightly to 494 cm^{-1} due to the presence of uncoordinated dtdb. Characteristic stretching bands for bipy (651 cm^{-1}) and phen (837 cm^{-1}) were found in complexes **2** and **3**, respectively. Chemical shifts arising from carbon and hydrogen atoms for the palladium complexes **2** and **3** concurred with the number and type of atoms present in their chemical environment. The aromatic protons were found to be in the range of 8.96–6.69 ppm in the ^1H NMR. The carboxylate carbons were found to be 168.4–167.6 ppm in the ^{13}C NMR spectra (see details in Section 3).

2.2. Structures of $[\text{Pd}(\text{tb})(\text{bipy})]\cdot 3\text{H}_2\text{O}$ (**1**) and $[\text{Pd}_2(\text{tb})_2(\text{bipy})_2]\cdot (\text{dtdb})_2$ (**2**)

The molecular structures of **1** and **2** are shown in Figs. 2 and 3, respectively, with selected bond lengths and bond angles tabulated in Table 2. Complex **1** crystallizes in an orthorhombic system, in which dtdb underwent reductive cleavage at the S—S bond, resulting in an OS donor chelate. The coordination geometry around the Pd atom in **1** is found to be square planar, coordinated to two nitrogens of bipyridine, sulfur and one oxygen of the carboxylic acid in a monodentate fashion, resulting in a PdN_2OS type of complex.

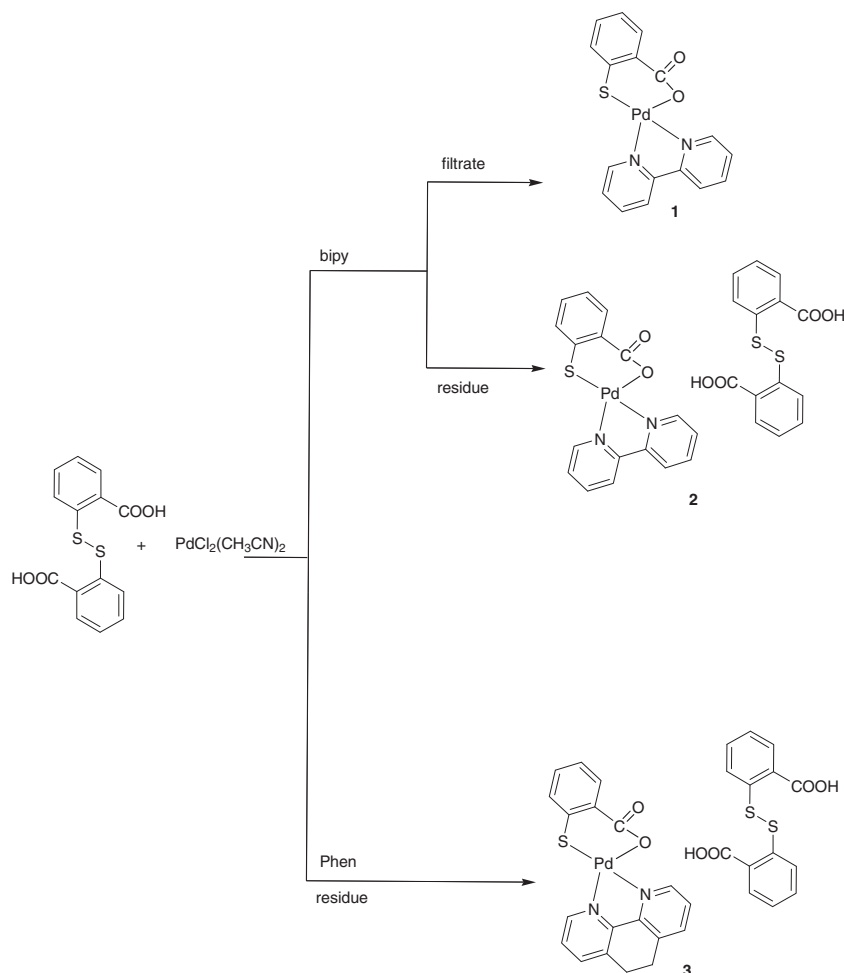
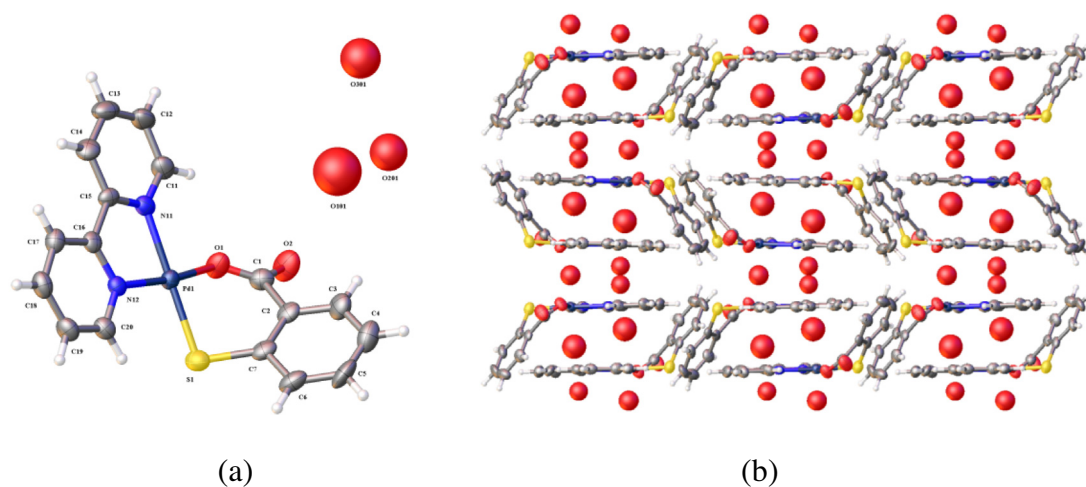


Figure 1 Synthesis of palladium complexes **1–3**.

Table 1 X-ray crystallography summary for structures **2** and **3**.

Identification code	2	3
Empirical formula	C ₄₈ H ₃₄ N ₄ O ₈ Pd ₂ S ₄	C ₅₂ H ₃₄ N ₄ O ₉ Pd ₂ S ₄
Formula weight	1135.83	1199.87
Temperature (K)	150	100
Wavelength (Å)	0.71075	0.71075
Crystal system	Triclinic	Triclinic
Space group	P1	P-1
<i>Unit cell dimensions</i>		
<i>a</i> (Å)	7.7767(5)	7.1189(7)
<i>b</i> (Å)	12.14444(9)	16.3221(11)
<i>c</i> (Å)	22.6509(16)	19.5842(13)
α (°)	87.646(4)	89.490(6)
β (°)	85.596(4)	84.409(6)
γ (°)	84.262(4)	84.780(7)
Volume (Å ³)	2121.0(3)	2255.4(3)
<i>Z</i>	2	2
ρ calc (mg/mm ³)	1.778	1.767
Absorption coefficient (mm ⁻¹)	1.109	1.050
<i>F</i> (000)	1140	1204
Crystal	Chip; red	Plate; yellow
Crystal size (mm ³)	0.06 × 0.06 × 0.01	0.08 × 0.03 × 0.02
θ range for data collection (°)	2.726–27.548	1.631–27.556
Reflections collected	28,315	19,891
Independent reflections	17,327	9676
Completeness to θ max (%)	99.7	94.7
Max and min transmission	1.000 and 0.714	1.000 and 0.201
Data/restraints/parameters	17,327/3/1193	9676/0/642
Goodness-of-fit on <i>F</i> ²	1.075	1.011
Final <i>R</i> indexes [<i>I</i> ≥ 2 σ (<i>I</i>)]	<i>R</i> 1 = 0.0537, <i>wR</i> 2 = 0.1538	<i>R</i> 1 = 0.0680, <i>wR</i> 2 = 0.1668
Final <i>R</i> indexes [all data]	<i>R</i> 1 = 0.0557, <i>wR</i> 2 = 0.1555	<i>R</i> 1 = 0.1288, <i>wR</i> 2 = 0.1984
Largest diff. peak/hole (e Å ⁻³)	2.316/−1.660	1.209/−1.762
CCDC deposition number/ref code	1401016	1401017

**Figure 2** (a) Asymmetric unit of **1** [Pd(tb)(bipy)]·3H₂O. Thermal ellipsoids are drawn at 50% probability level. (b) Packing structure of **1** showing hydrogen bonding.

The asymmetric unit of **1** comprised one independent molecule of complex **1** and three water molecules. The bipy ligand ring lies 57.0(4)° in relation to the split tb ligand ring both of

which are coordinated to the Pd atom. Bipy ligands stack on top of each other along crystallographic *c*. Every second bipy ligand is inverted. Disordered water channels are also observed

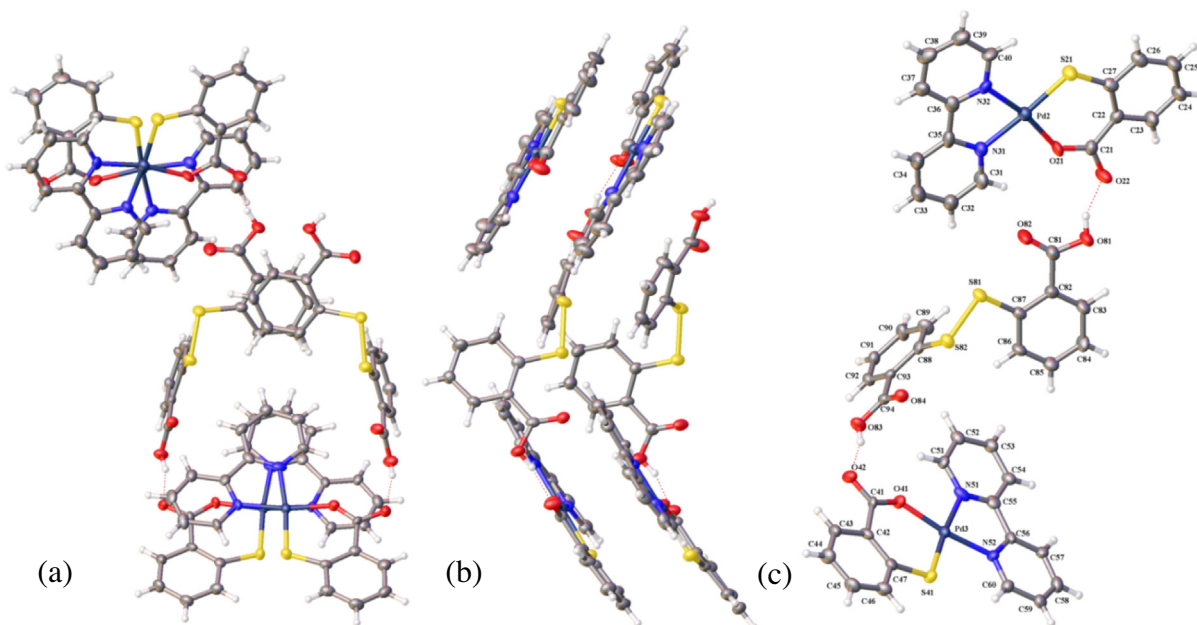


Figure 3 (a) Asymmetric unit of **2** $[\text{Pd}_2(\text{tb})_2(\text{bipy})_2]\cdot(\text{dtdb})_2$. Thermal ellipsoids are drawn at 50% probability level. (b) Viewed along crystallographic axis *b*. (c) Packing structure of **2** showing hydrogen bonding.

Table 2 Selected bond lengths (Å) and bond angles (°) for complexes **2** and **3**.

		2	3
<i>Pd bond distances (Å)</i>			
Pd–N(C)	Pd1–N11	2.053(9)	2.065(6)
	Pd1–N12	2.019(10)	2.029(6)
Pd–O(C)	Pd1–O1	1.996(9)	1.986(4)
Pd–S(C)	Pd1–S1	2.222(3)	2.227(2)
<i>Bond angles (°)</i>			
O–Pd–S	O1–Pd1–S1	93.8(2)	94.8(2)
O–Pd–N	O1–Pd1–N11	91.2(3)	90.7(2)
	O1–Pd1–N12	171.6(4)	172.0(2)
N–Pd–S	N11–Pd1–S1	174.9(3)	174.5(2)
	N12–Pd1–S1	94.6(3)	93.2(2)
N–Pd–N	N12–Pd1–N11	80.4(4)	81.4(2)
<i>Torsion angles (°)</i>			
C–S–S–C		–87.0(10)	96.1(11)

along crystallographic axis *c*. Although these water molecules are disordered it appeared that they formed hydrogen bonds with the uncoordinated oxygen of the carboxylate from the split *tb* ligand.

Complex **2** is found to crystallize in a triclinic system. However, it is found to possess similar PdN_2OS coordination environment as in **1**, with the Pd being in a square planar geometry and deviating from the ideal perfect square planar system (80.4(4)–94.6(3)) [17]. The bond lengths of Pd–N (2.053(9)–2.019(10) Å), Pd–O (1.996(9) Å) and Pd–S (2.222(3) Å) differ slightly from complex **1** [Pd–N (2.063(6)–2.020(5) Å), Pd–O (2.007(5) Å) and Pd–S (2.262(2) Å)], but are still within the range reported for other Pd complexes [21,28]. However, the striking feature of **2** is the presence of the organic dtdb, which

has crystallized in the triclinic system with space group P1. The bipy ligand in complex **1** lies 57.0(4)° to the *tb*, while that in complex **2** lies along the same plane. The atomic arrangement of the non-symmetric cluster can be described by the alternation of the inorganic–organic layers, connected by hydrogen bonding interactions between the uncoordinated oxygen of the complex and hydrogen atom of dtdb (O81–H81···O22 = 2.519(12) Å, O83–H83···O42 = 2.507(10) Å, O101–H101···O2 = 2.522(12) Å, O103–H103···O62 = 2.478(11) Å). The complexes do appear to stack on top of one another but not in the same way as described in complex **1**. The bipy ligands do not stack directly but they are offset.

2.3. Structure of $[\text{Pd}_2(\text{tb})_2(\text{phen})_2]\cdot\text{dtdb}\cdot\text{H}_2\text{O}$ (**3**)

Complex **3** is found to crystallize in a triclinic system, P-1. The dtdb ligand was split into two *tb*'s after scission about the S–S bond and the *tb* anion coordinated to the palladium atom via its carboxylate oxygen and sulfur. The palladium atom was further coordinated to two nitrogens of the phenanthroline unit to complete the square planar geometry. The presence of the unreacted dtdb was also observed in complex **3** (Fig. 4). The arrangements of the phen ligands with respect to the split *tb* ligand were the same as seen within complex **2** where the ligands lie across the same plane. Fig. 5 shows the supramolecular trimer formed via hydrogen bonding of the uncoordinated carboxylate oxygen of the complex and the hydrogen atoms of dtdb (O61–H61···O32 = 2.502(7) Å, O63–H63···O2 = 2.521(8) Å). The main difference in packing arrangements is due to the additional incorporation of water within the structure which forms within a channel along crystallographic axis *a*. The stacking arrangement bears most similarity to complex **2**. However, the phen ligand is completely offset causing the phen ligands to stack on top of split *tb* ligands and *tb* ligands to lie on top of phen ligands.

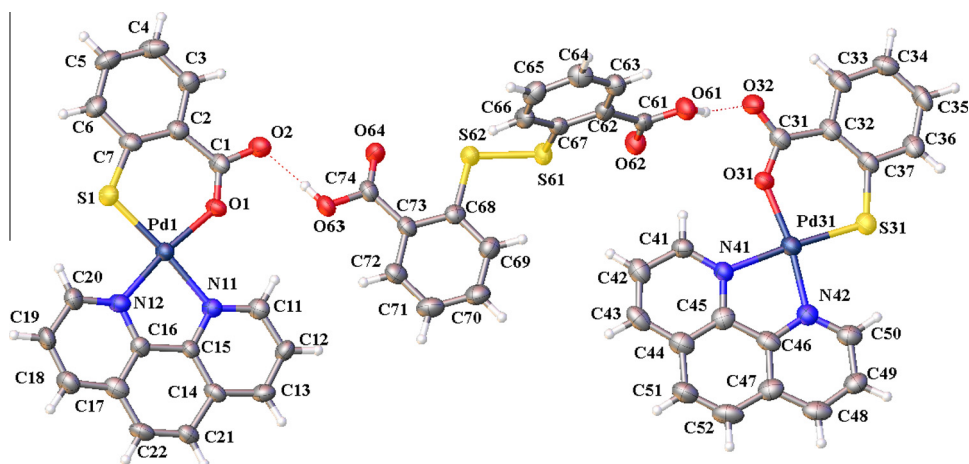


Figure 4 Asymmetric unit of 3 ($[\text{Pd}_2(\text{tb})_2(\text{phen})_2] \cdot \text{dtdb} \cdot \text{H}_2\text{O}$). Thermal ellipsoids are drawn at 50% probability level. Solvent water molecules are omitted for clarity.

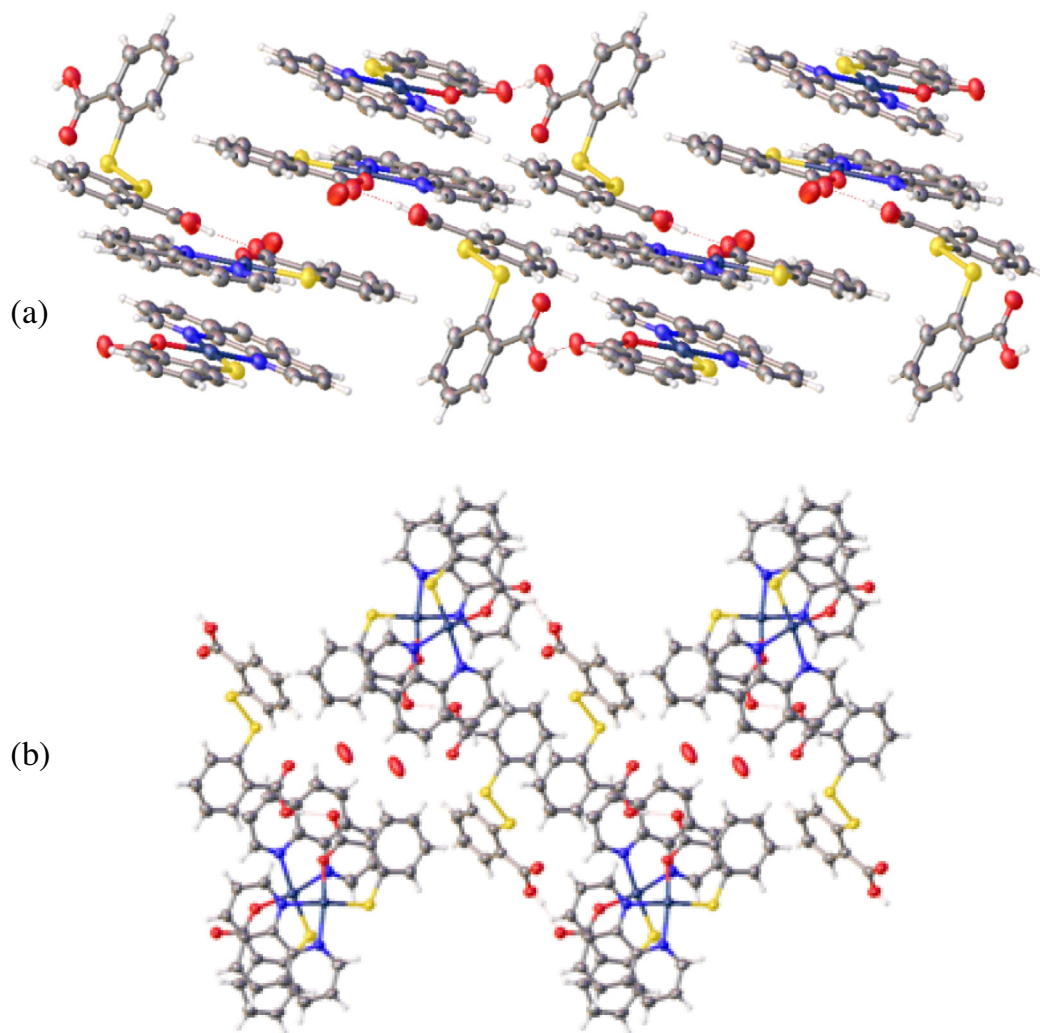


Figure 5 The X-ray crystal structure packing of 3 ($[\text{Pd}_2(\text{tb})_2(\text{phen})_2] \cdot \text{dtdb} \cdot \text{H}_2\text{O}$), (a) packing viewed down crystallographic axis c , (b) packing viewed down crystallographic axis a .

2.4. Catalytic behavior toward Heck reaction

Complexes **1–3** were investigated as catalysts in the Heck coupling reactions of iodobenzene with methyl acrylate (Fig. 6). A meticulous view on the C–C coupling process reveals that reaction conditions such as solvent, base and temperature are known to affect yields of the Mizoroki–Heck reaction products [25]. The conversion of iodobenzene in the presence of different bases catalyzed by **1** at 120 °C was monitored and the results are tabulated in Table 3. In the present study, a stoichiometric amount (0.54 mol%) of complex **1** is used to ascertain high conversions of the Heck cross-coupling as it is known that high catalyst loading inhibits the catalytic reaction [29].

According to previous reports, the N,N'-dimethylacetamide (DMA) was found to be the preferred solvent, leading to the formation of the Heck products in excellent yield even at low temperature [2]. Hence, we chose this solvent in our system, but surprisingly, no product was formed. When the solvent was changed to DMF, 44% of the cinnamate was obtained (entry 2). This clearly proved that a catalyst has high activity only in a specific solvent. The reaction was found to be time dependent. Increasing the reaction from 46 to 69 h caused a remarkable increase in the yield of the product (entries 2 and 3). However, when the reaction time was increased to 93 h, the yield of the product was found to decrease slightly. Thus, all the other experiments were carried out at 69 h. When other



Figure 6 Heck reaction between iodobenzene and methyl acrylate.

Table 3 Optimization of reaction conditions for iodobenzene and methyl acrylate.

Entry	Base	Solvent	Catalyst	Time (h)	% Yield
1	K ₂ CO ₃	DMA	1	69	No reaction
2	K ₂ CO ₃	DMF	1	46	44
3	K ₂ CO ₃	DMF	1	69	74
4	K ₂ CO ₃	DMF	1	93	60
5	Na ₂ CO ₃	DMF	1	69	37.8
6	CsCO ₃	DMF	1	69	36.9
7	Et ₃ N	DMF	1	69	11.3
8	K ₂ CO ₃	DMF	1	69	68 ^a
9	K ₂ CO ₃	DMF	1	69	68 ^b
10	K ₂ CO ₃	DMF	1	69	No reaction ^c
11	K ₂ CO ₃	DMF	2	69	12
12	K ₂ CO ₃	DMF	3	69	Trace
13	K ₂ CO ₃	DMF	PdCl ₂ /dtdb	69	29
14	K ₂ CO ₃	DMF	–	69	Trace ^d

^a Under N₂ atmosphere.

^b Catalyst used = 0.024 mmol.

^c Reaction was carried at 25 °C.

^d No catalyst.

bases such as Na₂CO₃ (entry 5), CsCO₃ (entry 6) and Et₃N (entry 7) were employed, the product was obtained in low yield. Subsequently, the reaction was carried out under N₂ atmosphere to improve the yield of methyl cinnamate. However, no change was observed, even though the catalyst loading was increased from 0.54 to 0.76 mol% (entry 9). These observations are consistent with the results obtained by Vries [29] on the appropriate amount to effectively convert substrates into Heck products. It is worth mentioning here that we have been able to catalyze the C–C cross coupling reaction successfully, achieving a yield up to 74%, using a very low % of catalyst loading as compared to other reports [24]. When the reaction was carried out at ambient temperature, no product was formed (entry 10). Complexes **2** and **3** were also screened for their catalytic behavior toward Heck reaction, but were found to be inefficient. A 1:1 ratio of complex **1** and dtdb gave only 5% of the methyl cinnamate. Hence it could be deduced that the presence of the uncoordinated dtdb hindered the activity of the complexes. An *in situ* reaction of PdCl₂/dtdb in the Heck reaction provided no increase in the outcome of the reaction, highlighting the importance of complex **1** as catalyst (entry 13). A controlled experiment indicated that a small amount of the cross coupling product was observed in the absence of the catalyst (entry 14). We were not able to recover the catalyst despite various attempts to do so.

2.5. Antibacterial activity

Dtdb and complex **1** were screened for their antibacterial activities against *Staphylococcus aureus* (ATCC 25923), *Staphylococcus epidermis* (ATCC 12228), *Bacillus cereus* (ATCC 10876) and *Salmonella typhimurium* (ATCC 14028) using the microbroth dilution method. Complex **1** was found to exhibit more inhibitory effect compared to the parent ligand dtdb and standard erythromycin (Table 4). The increase in activity might be explained using the concept of chelation theory [22], which relates lipophilicity with antibacterial property. The metal positive charge in a complex is partially shared with the ligand upon coordination and hence increases the delocalization of π -electrons over the whole chelate ring, favoring the lipophilic character of the metal complexes. This enhanced lipophilicity increases the penetration of the complex into the lipid layer of the bacterial cell membranes, disrupting the metal binding sites in enzymes of microorganisms. In addition, the complex might also disturb the respiration process and the synthesis of proteins, which restricts further growth of microorganisms. The compounds were also found to be more toxic against the Gram positive strains (*S. aureus*, *S. epidermidis*, *B. cereus*) as compared to Gram negative *S. typhimurium*. This trend in activity could be due to the higher antigenic properties of Gram negative bacteria, which are known to possess an outer lipid membrane of lipopolysaccharides, making them more resistant to antibacterial agents.

Table 4 MIC of dtdb and complex **1** (μ M).

Bacteria	dtdb	1	Erythromycin
<i>S. aureus</i> (ATCC 25923)	1990	9.89	850
<i>S. epidermis</i> (ATCC 12228)	9950	9.89	≤1.4
<i>B. cereus</i> (ATCC 10876)	9950	9.89	3
<i>S. typhimurium</i> (ATCC 14028)	7960	83.3	213

2.6. Antioxidant activity

The DPPH assay was used to evaluate the antioxidant activity of the compounds due to its simple procedure and reliability [15]. A lower IC₅₀ value reflects better DPPH radical-scavenging activity. Complex **1** showed better activity compared to dtdb (IC₅₀ = 204 ± 2 μM) and ascorbic acid (IC₅₀ = 2800 ± 2 μM) with an IC₅₀ 55.1 ± 0.031 μM. The high activity obtained for the metal complexes showed that the combination of metal with ligand plays a vital role in the development of an effective antioxidant.

3. Experimental section

3.1. General procedure and materials

Dithiosalicylic acid, 2,2'-bipyridine and 1,10-phenanthroline were bought from Sigma Aldrich (Germany, UK). Palladium (II) chloride was obtained from Alpha Chemika (England). DMF and methanol were purchased from Qualichems (India) and Lobachemie (India), respectively. Iodobenzene and methyl acrylate were purchased from BDH (England) and Acros, respectively. 1,1-diphenyl-2-picrylhydrazyl and iodonitrotetrazolium chloride (INT) were purchased from Aldrich (USA) while ascorbic acid and Mueller–Hinton broth were bought from Loba Chemie (India) and Oxoid Ltd (UK) respectively. The different bacterial strains were obtained from Microbiologics® (St Cloud, MN, USA) and Oxoid Ltd (United Kingdom). Melting points of the samples were determined using a Stuart Scientific Electronic IA 9100 melting point apparatus and were uncorrected. Infrared spectroscopy on a diamond smart accessory was recorded on a Bruker Alpha FTIR spectrometer in the range 400–4000 cm⁻¹ on a diamond cell. ¹H and ¹³C NMR spectra were recorded at 250 and 62.9 MHz respectively on a Bruker spectro spin NMR spectrometer using DMSO. Carbon, hydrogen, nitrogen, and sulfur contents were obtained from a Eurovector EA 3000 elemental analyzer. Conversions were determined by Perkin Elmer Clarus 500/560S GC–MS equipped with a 30 m × 0.32 mm × 0.5 μm film thickness BPX5 capillary column.

3.2. Synthesis of palladium complexes (1–3)

PdCl₂·2H₂O was refluxed in anhydrous acetonitrile to generate PdCl₂(CH₃CN)₂. A mixture of dtdb (0.214 g, 0.700 mmol) and bipy/phen (0.700 mmol) in DMF (5 ml) was carefully layered onto a solution of PdCl₂(CH₃CN)₂ (0.182 g, 0.700 mmol) in 5 ml of DMF and 5 ml of MeOH. The pH of dtdb was adjusted to pH 7.2 using 1 M NaOH solution. The resulting mixture was kept at room temperature. After 8 weeks, the solution was decanted to isolate reddish-brown complex **2**. The red solution obtained was concentrated and red crystals of **1** were obtained after a few days. Orange microcrystalline solid of **3** was obtained from the mixture of dtdb and phenanthroline after a few days.

2: % yield: 10%. m.p.: > 250 °C. IR (cm⁻¹): 1667 (C=O), 1601 (C=O) 1585, 1557, 1433, 1366, 647, 495 (S–S), 448 (Pd–N). ¹H NMR δ ppm (DMSO): 8.94 (*d*, 2H, *J* = 5 Hz, CH–N), 8.74 (*d*, 2H, *J* = 4 Hz, bipy), 8.71 (*d*, 2H,

J = 4 Hz, UL), 8.49 (dd, 2H, *J* = 4, 4.5 Hz, bipy), 8.43 (*d*, 1H, *J* = 8 Hz, CL), 8.08 (dd, 2H, *J* = 6.5, 8 Hz, UL), 7.99 (*d*, 2H, *J* = 8 Hz, UL), 7.90 (dd, 2H, *J* = 4, 6.5 Hz, UL), 7.53 (*d*, 1H, *J* = 7.4 Hz, CL), 7.25 (2 *t* merging, 2H, *J* = 7.4 Hz, CL), 7.13 (*t*, 2H, *J* = 5, 4.5 Hz, bipy). ¹³C NMR δ ppm (DMSO): 168.4 (C=O), 168.1 (C=O), 157.3 (C–C=N), 154.1 (C–C=N), 149.4 (C=N), 145.5 (C=N), 142.9, 141.4, 139.5, 134.4, 133.8, 133.2, 132.1, 129.5, 128.6, 128.0, 126.5, 125.5, 124.7, 123.8, 122.9. Anal. Calcd. for C₄₈H₃₄N₄O₈Pd₂S₄: C, 50.75; H, 3.02; N, 4.93; S, 11.29. Found: C, 51.60; H, 2.99; N, 5.39; S, 11.35.

3: % yield: 45%. m.p.: 250 °C. IR (cm⁻¹): 1665 (C=O), 1619 (C=O), 1586, 1562, 1568, 1426, 839, 524 (Pd–O), 494 (S–S). ¹H NMR δ ppm (DMSO): 8.95 (*d*, 2H, *J* = 5 Hz, phen), 8.87 (*d*, 2H, *J* = 4.3 Hz, phen), 8.81 (*d*, 2H, *J* = 5 Hz, UL), 8.23–8.15 (*m*, 3H, phen, CL), 8.11 (*d*, *J* = 4, 7.8 Hz, 1H, UL), 8.01, 7.98 (dd, 2H, *J* = 4.3, 5.4 Hz, phen), 7.94 (*d*, 2H, *J* = 7.8 Hz, UL), 7.40 (*d*, 2H, *J* = 7.4 Hz, CL), 7.14 (dd, 2H, *J* = 4, 5 Hz, UL), 7.01 (*t*, 2H, *J* = 7.4 Hz, CL). ¹³C NMR δ ppm (DMSO): 167.9 (C=O), 167.6 (C=O), 149.4 (C=N), 147.0 (C=N), 145.7 (C–C=N), 144.3 (C–C=N), 142.3 (CL), 139.9 (phen), 139.4 (UL), 138.9 (UL), 134.0 (UL), 133.2 (CL), 132.9 (phen), 131.5 (UL), 130.4 (UL), 129.8 (phen), 128.9 (UL), 127.4 (CL), 126.1 (CL), 124.9 (CL), 122.4 (CL). Anal. Calcd. for C₅₂H₃₄N₄O₈Pd₂S₄: C, 52.75; H, 2.89; N, 4.73; S, 10.83. Found: C, 52.60; H, 2.58; N, 4.98; S, 11.05

CL = coordinated ligand, UL = uncoordinated ligand.

3.3. X-ray crystallography

Single-crystal X-ray diffraction data for **1** were collected on a Rigaku XtaLab mini benchtop diffractometer with a sealed tube generator operating at 600 W (50 kV, 12 mA), a SHINE curved graphite monochromator (MoKα₁/Kα₂ = 0.71073 Å) and a 0.8 mm collimator. A 2 circle goniometer with a Mercury 3 CCD detector was used to collect the asymmetric unit of data using phi scans with a fixed crystal-to-detector distance of 50 mm, fixed chi of 54° and a fixed 2θ of 30°. Data for **2** and **3** were collected on a Rigaku AFC12 goniometer equipped with an enhanced sensitivity (HG) Saturn 724+ detector mounted at the window of an FR–E+ Superbright Mo Kα rotating anode generator with optics VHF Varimax 70 μm focus and equipped with an Oxford CryosystemsCobra [4] cooling device. Data for **1** were collected at 170 K, **2** at 150 K and **3** at 100 K.

Cell determination, data collection, data reduction, cell refinement and absorption corrections were carried out using CrystalClear-SM Expert 3.1 b27 software [23]. Structures **1–3** were solved using Superflip [6]. All structures were refined using full-matrix least-squares refinements in the SHELX2013 software [19]. All non-hydrogen atoms were refined with anisotropic displacement parameters. All hydrogen atoms were added at calculated positions and refined using a riding model with isotropic displacement parameters based on the equivalent isotropic displacement parameter (U_{eq}) of the parent atom. Hydrogen atoms of water molecules O101 within **3** could not be located. Figs. 1–3 were drawn using Olex2 [26].

3.4. Heck reaction

A sealed tube containing 3 mmol of iodobenzene, 4 mmol of methyl acrylate, 4.5 mmol (K_2CO_3), and 0.0052 mmol of complex was heated at 120 °C in DMF for 69 h. The samples were diluted in DCM and were analyzed by GC to determine the percentage conversions. The coupling product was isolated by extracting with diethyl ether to give a pure product which was confirmed by NMR spectroscopy. Octadecane was used as the internal standard.

3.5. Antioxidant assay

DPPH solution (100 μ M, 200 μ L) was added to the compounds and 100 μ L of the solution was placed in each well of an ELISA 96 well plate. After 30 min of incubation at 40 °C, the absorbance of the solutions was measured at wavelength of 492 nm using a Labsystems Multiskan Ms EIA Reader. The experiment was performed in duplicate. Ascorbic acid was used as the positive control (PC). The experiments were carried out using spectroscopic grade methanol solvent at 298 K. The 50% scavenging concentration (IC_{50}) was based on the amount of compound required to decrease the initial DPPH radical concentration by 50% and was calculated using Growth formula in Microsoft Excel and expressed as mean \pm standard deviation (SD).

The percentage radical scavenging activity of the tested compounds, expressed as percentage inhibition DPPH, was calculated according to the formula:

$$\% \text{ Inhibition} = [(A_0 - A_s)/A_0] \times 100$$

where A_s = difference in absorbance of the tested sample after adding DPPH (after incubation) and before adding DPPH, A_0 = absorbance of the blank sample.

For the antioxidant assays, all the results were done in triplicate and expressed as mean \pm standard deviation (SD).

3.6. Antibacterial

Minimum Inhibition Concentration (MIC) was found out by the broth dilution method [10]. Standardized Inoculum (matched to McFarland $BaSO_4$ solution) of suspension of organisms was prepared. 100 μ L of the Mueller–Hinton broth was placed in each well of an Elisa 96 well plate followed by serial dilution of the tested compound. 100 μ L of the bacterial strain was then added to each well and placed in an incubator at 40 °C for 24 h. 40 μ L of INT (0.4 mg/mL) was then placed in each well and incubated for 0.5 h. The change in color was then noted and the MIC was taken as the lowest concentration in which no color change was observed. Erythromycin, which is known to possess a broad spectrum of activity, was used as standard and DMSO as negative control, where no sample was present.

4. Conclusions

The present work shows that dtdb underwent S–S cleavage upon reacting with $PdCl_2(CH_3CN)_2$ in the presence of phen and bipy leading to square planar complexes. The presence of trapped uncoordinated ligand in complexes **2** and **3** was

confirmed by X-ray study. The square planar palladium complexes were evaluated for their catalytic activities in the coupling of iodobenzene with methyl acrylate. The reactions were found to be strongly dependent on a number of factors such as base, catalyst loading, solvent, temperature, time and the combined effect of these. Complex **1** exhibited better catalytic activity compared to complexes **2** and **3**. Complex **1** was found to possess a broad spectrum of antibacterial activity, showing MIC of 9.89 μ M. Moreover, complex **1** was found to scavenge the free radicals more effectively compared to the standard and free ligand.

Acknowledgement

One of the authors is thankful to Tertiary Education of Mauritius for grant of Scholarship.

Appendix A. Supplementary data

Supplementary data associated with this article can be found, in the online version, at <http://dx.doi.org/10.1016/j.jscs.2015.10.003>.

References

- [1] O.A. Akrawi, A. Khan, M. Hussain, H.H. Muhammad, A. Villinger, P. Langer, Synthesis of 2,3-diarylfuorenones by domino 'twofold Heck/electrocyclization/dehydrogenation' reactions of 2,3-dibromoindenone, *Tetrahedron Lett.* 54 (2013) 3037–3039.
- [2] M. Bagherzadeh, F. Ashouri, L. Hashemi, A. Morsali, Supported Pd nanoparticles on Mn-based metal–organic coordination polymer: efficient and recyclable heterogeneous catalyst for Mizoroki–Heck cross coupling reaction of terminal alkenes, *Inorg. Chem. Commun.* 44 (2014) 10–14.
- [3] S. Balboa, R. Carballo, A. Castiñeiras, J.M. González-Pérez, J. Nicolás-Gutiérrez, Structural features of palladium(II) complexes with α -hydroxycarboxylate and aromatic α,α' -diimine ligands, *Polyhedron* 50 (2013) 512–523.
- [4] I.P. Beletskaya, A.V. Cheprakov, The heck reaction as a sharpening stone of palladium catalysis, *Chem. Rev.* 100 (2000) 3009–3066.
- [5] W. Chen, C. Xi, Y. Wu, Highly active Pd(II) catalysts with pyridylbenzoimidazole ligands for the Heck reaction, *J. Organomet. Chem.* 692 (2007) 4381–4388.
- [6] S.J. Coles, P.A. Gale, Changing and challenging times for service crystallography, *Chem. Sci.* 3 (2012) 683–689.
- [7] D.K. Demertzi, P.N. Yadav, M.A. Demertzi, J.P. Jasiski, F.J. Andreadaki, I.D. Kostas, First use of a palladium complex with a thiosemicarbazone ligand as catalyst precursor for the Heck reaction, *Tetrahedron Lett.* 45 (2004) 2923–2926.
- [8] A. Fihri, P. Meunier, J. Hierso, Performances of symmetrical achiral ferrocenylphosphine ligands in palladium–catalyzed cross-coupling reactions: a review of syntheses, catalytic applications and structural properties, *Coord. Chem. Rev.* 251 (2007) 2017–2055.
- [9] E. Gao, F. Guan, X. Gao, M. Zhu, L. Liu, C. Wang, W. Zhang, Y. Sun, Novel palladium(II) complexes containing a sulfur ligand: structure and biological activity on HeLa cells, *J. Biol. Inorg. Chem.* 17 (2012) 263–274.
- [10] R. Hakasa, K. Turecka, C. Orlewska, W. Werel, Comparison of fluorescence optical respirometry and microbroth dilution methods for testing antimicrobial compounds, *J. Microbiol. Methods* 107 (2014) 98–105.

- [11] Y. Heo, Y.Y. Kang, T. Palani, J. Lee, Synthesis, characterization of palladium hydroxysalen complex and its application in the coupling reaction of arylboronic acids: Mizoroki–Heck type reaction and decarboxylative couplings, *Inorg. Chem. Commun.* 23 (2012) 1–5.
- [12] W.A. Hermann, C.P. Reisinger, M. Spiegler, Chelating *N*-heterocyclic carbene ligands in palladium-catalyzed heck-type reactions, *J. Organomet. Chem.* 557 (1998) 93–96.
- [13] S. Hermans, M. Wenkin, M. Devillers, Carboxylate-type palladium(II) complexes as soluble precursors for the preparation of carbon-supported Pd/C catalysts, *J. Mol. Catal. A Chem.* 136 (1998) 59–68.
- [14] M. Keleş, H. Keleş, D.M. Emir, Pd(II) complexes of Schiff bases and their application as catalysts in Mizoroki–Heck and Suzuki–Miyaura cross-coupling reactions, *Appl. Organomet. Chem.* 14 (2015) 543–548, <http://dx.doi.org/10.1002/aoc.3329>.
- [15] M. Kumar, T. Padmini, K. Ponnuvel, Synthesis, characterization and antioxidant activities of Schiff bases are of cholesterol, *J. Saudi Chem. Soc.* (2014), <http://dx.doi.org/10.1016/j.jscs.2014.03.006>.
- [16] Z.D. Matović, E. Mrkalić, G. Bogdanović, V. Kojić, A. Meetsma, R. Jelić, Antitumor effects of a tetradentate amidocarboxylate ligands and corresponding square-planar palladium (II) complexes toward some cancer cells. Crystal structure, DFT modeling and ligand to DNA probe Docking simulation, *J. Inorg. Biochem.* 12 (2013) 134–144.
- [17] N. Miklášová, E. Fischer-Fodor, R. Mikláš, L. Kucková, J. Kožisek, T. Liptaj, O. Soritau, J. Valentová, F. Devínsky, Synthesis and characterization of new biologically active palladium(II) complexes with (1*E*,6*E*)-1,7-bis(3,4-diethoxyphenyl)-1,6-heptadiene-3,5-dione, *Inorg. Chem. Commun.* 46 (2014) 229–233.
- [18] S. Moosun, L.H. Blair, S.J. Coles, S. Jhaumeer-Laulloo, M.G. Bhowon, Novel copper(II) thiodibenzoic acid coordination polymers by in situ extrusion of sulfur from 2,2-dithiodibenzoic acid and the unique oxidation of disulfide to sulfate, *Z. Anorg. Allg. Chem.* 641 (2015) 890–895.
- [19] L. Palatinus, G. Chapuis, SUPERFLIP – a computer program for the solution of crystal structures by charge flipping in arbitrary dimensions, *J. Appl. Crystallogr.* 40 (2007) 786–790.
- [20] P. Pelagatti, M. Carcell, M. Costa, S. Ianelli, C. Pelizzi, D. Rogolina, Heck reaction catalysed by pyridyl-imine palladium (0) and palladium(II) complexes, *J. Mol. Catal. A Chem.* 226 (2005) 107–110.
- [21] G.P. Radic, V.V. Glodovic, I.D. Radojevic, O.D. Stefanovic, L. R. Comic, Z.R. Ratkovic, A. Valkonen, K. Rissanen, S.R. Trifunovic, Synthesis, characterization and antimicrobial activity of palladium(II) complexes with some alkyl derivatives of thiosalicylic acids: crystal structure of the bis(*S*-benzylthiosalicylate)–palladium(II) complex, [Pd(*S*-bz-thiosal)₂], *Polyhedron* 31 (2012) 69–76.
- [22] N. Raman, A. Kulandaisamy, A. Shunmugasundaram, K. Jayasubramanian, Synthesis, spectral, redox and antimicrobial activities of Schiff base complexes derived from 1-phenyl-2,3-dimethyl-4-aminopyrazol-5-one and acetoacetanilide, *Transition Met. Chem.* 26 (2001) 131–135.
- [23] Rigaku, CrystalClear-SM Expert 3.1 b27, 2013.
- [24] S.J. Sabounchei, M. Ahmad, Palladacycle phosphine complexes as homogeneous catalysts for the Heck cross-coupling reaction at low catalyst loading under aerobic conditions, *Inorg. Chim. Acta* 405 (2013) 15–23.
- [25] T.M. Shaikh, C. Weng, F. Hong, Secondary phosphine oxides: versatile ligands in transition metal-catalyzed cross-coupling reactions, *Coord. Chem. Rev.* 256 (2012) 771–803.
- [26] G. Sheldrick, A short history of SHELX, *Acta Crystallogr. Sect. A Found. Crystallogr.* 64 (2008) 112–122.
- [27] N. Smrecki, B. Kukovec, J. Jazwinski, Y. Liu, J. Zhang, A. Mikecin, Z. Popovic, Preparation and characterization of palladium(II) complexes with *N*-arylalkyliminodiacetic acids. Catalytic activity of complexes in methoxycarbonylation of iodobenzene, *J. Organomet. Chem.* 760 (2014) 224–230.
- [28] E. Tomás-Mendivil, J. Díez, V. Cadierno, Palladium(II) complexes with symmetrical dihydroxy-2,2'-bipyridine ligands: exploring their inter- and intramolecular interactions in solid-state, *Polyhedron* 59 (2013) 69–76.
- [29] G. Vries, A unifying mechanism for all high-temperature Heck reactions. The role of palladium colloids and anionic species, *Dalton Trans.* (2006) 421–429.